Asian Journal of Chemistry; Vol. 35, No. 2 (2023), 475-482

ASIAN JOURNAL OF CHEMISTRY

https://doi.org/10.14233/ajchem.2023.26947

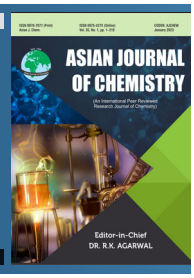

Influence of *Pongamia pinnata* Leaf Extract based Silver Nanoparticles Towards the Degradation of Safranin O Dye

A. Alvin Kalicharan[1,*], V. Anbarasan[2], R. Priyanka[3] and K. Arivalagan[4]

[1]Department of Chemistry, Panimalar Engineering College, Chennai-600123, India
[2]Department of Chemistry, DMI College of Engineering, Chennai-600123, India
[3]Department of Chemistry, Dr. Ambedkar Government Arts College, Chennai-600039, India
[4]Department of Chemistry, Government Arts College for Men(A), Chennai-600035, India

*Corresponding author: E-mail: kalicharan19982@gmail.com

Received: 19 November 2022; *Accepted*: 9 January 2023; *Published online*: 30 January 2023; AJC-21133

Use of medicinal herbs for green synthesis of nanoparticles has attracted researchers owing to their valuable influence on mankind. Benefit of consuming plants aimed at greener production of nanomaterials relies on the less toxicity and cost-effective protocol. Herein, we reported the synthesis of biocompactible silver nanoparticles using *Pongamia pinnata* leaf extract. The biomolecules existing in leaf extract of *Pongamia pinnata* played dual role for capping and equilibrium of silver nanoparticles. Phenomena of surface plasmon resonance was observed from the UV-Vis spectrum around 426 nm. The FTIR peaks revealed the significance of biomolecules in the formation of stable silver nanoparticles. From XRD pattern, peaks attained has better covenant with Ag in metal form with face-centered-cubic feature. Morphology of silver nanoparticles from SEM and TEM studies revealed that the particles are spherical in shape. Degradation of safranin O dye using green synthesized silver nanoparticles exhibited better degradation efficiency. Without much advent process, this method for synthesizing silver nanoparticles provides an inexpensive and environmentally responsible approach.

Keywords: *Pongamia pinnata*, Green synthesis, Silver nanoparticles, Safranin O, Photocatalytic degradation.

INTRODUCTION

In the modern era, the most difficult task on the planet is to provide safe and clean drinking water, which is a basic human need and an essential asset of life on Earth. Despite, more mandate and less water resources, it has directed to an investigation of novel technologies for satisfying water supplies. Dye effluents from several industries are the main source for water pollution in the earth which ultimately causes many health hazards in human beings and aquatic animals. These larger dye molecules are the causative for acidification, reduction in oxygen content, transmission of cancer causing agents and causes several diseases [1,2]. Among different dyes, safranin O is an alkaline dye and mostly utilized as colouring agent in food products, dying agent for thread, flax, leather, fleece, ply and wrapper and in production of pigment and indelible inks. Excess exposure of this dye causes several health hazards [3].

Several attempts were made for past few decades for the degradation of dye effluents through chemical and physical methods like coalescence, activated carbon adsorption and bacterial treatment. Still, these techniques has some drawbacks that hinders their extensive recognition [4].

Traditionally, silver is a better recognized metal for its excellent antimicrobial properties, chemical stability, conductivity and catalytic behaviour which marks them to be more suitable for multiple applications, especially as durable adsorbent for the degradation of several dyes [5]. With the advent of nanotechnology, for past decades silver nanoparticles (AgNPs) have influenced a lot in the field of environmental remediation for wastewater cleanup [6]. Owing to the unique characteristics of AgNPs namely great superficial to size proportion, varied morphology, concordant optical possessions and lesser size makes them a suitable candidate for degradation of dyes [7]. Among various methods for synthesis of AgNPs, green synthesis using plant parts are of supreme important owing to the less toxicity and eco-friendly approach [8].

Pongamia pinnata is predominantly found in several parts of the World and it is a versatile leguminous tree consisting

various phytoconstituents. It has enriched basis of ores, amino groups, likewise encompasses peripheral metabolites. It comprises great nutritive worth consisting larger and smaller nutrients as a special manure in farming. Its leaves juices help to treat leprosy, diarrhoea, dry coughs, gonorrhoea, flatulence and colds [9,10]. In this research work, the silver nanoparticles were synthesized *via* a green route using leaf extract of *Pongamia pinnata* and silver nitrate solution. Here, the herbal extracts reduced metallic Ag ions through a process including capping and tumbling. The synthesized AgNPs were analyzed with ultraviolet-visible (UV-Vis), Fourier transform infrared (FTIR), powder X-ray diffraction (XRD), dynamic light scattering (DLS), scanning electron microscopy (SEM), transmission electron microscopy (TEM) and selected area electron diffraction (SAED) methods for its optical, structural, morphological and lattice parameter analysis. Furthermore, the synthesized AgNPs was also applied in the degradation of safranin O dye under optimized conditions.

EXPERIMENTAL

All the compounds utilized in following experimentation were procured from Sigma-Aldrich and used without further purification. A 0.1 M solution of silver nitrate was prepared using milli Q. water with high purity.

Preparation of *Pongamia pinnata* leaf extract: Fresh *Pongamia pinnata* leaves were collected locally and then washed thoroughly with tap water followed by distilled water. After dried for 5 to 10 days at room temperature in a covered area, the dry leaves were pulverized in an electronic blender and then stored the fine powder at room temperature. In 250 mL of conical flask, 10 g of leaf extract powder was mixed with 100 mL of Millipore water followed by heating at 80 ºC for 0.5 h. Filtered the pale brown colour liquid extract using Whatman filter paper No. 1 and then adjusted the pH of the solution to 11 using 0.1 M of NaOH solution [11].

Synthesis of silver nanoparticles: *Pongamia pinnata* leaves extract (50 mL) was added to 100 mL of 0.1 M $AgNO_3$ at room temperature in a conical flask under static condition. As soon as AgNPs formed, the colour changes after pale brownish to reddish-brown. Then, the solution was centrifuged to obtain the precipitate and then dehydrated in an oven at 100 ºC for 24 h [12].

Characterization: To examine the optical properties of the green synthesised AgNPs, a UV-Visible spectrophotometer (Elico SL210) was monitored between 200 and 650 nm. The functional groups present in the AgNPs were analyzed by Fourier transform infrared spectrophotometer (Perkin-Elmer) in the range of 4000 and 400 cm^{-1}. The nature of the particles was studied using X-Ray diffractometer (D8 Bruker Advance) using Cu$K\alpha$ radiation at a scan rate of 0.02º/min with constant time of 2 min. Particle size in colloidal dispersion was measured using dynamic light scattering particle size analyzer (Spectroscatter 201). The morphology of the synthesized AgNPs was elucidated from the scanning electron microscopy (JEOL-6390LA) and transmission electron microscopy (JEOL-JEM 2100) fortified along selected area electron diffractometer.

Degradation of safranin O dye: *Pongamia pinnata* leaf extract based AgNPs were utilized for the adsorption studies to decolourize safranin O dye. The green synthesized AgNPs were added to dye molecule and shaken well in a stirrer. Finally the optical measurements was measured in UV-Visible spectrophotometer to evaluate the adsorption effect. Different parameters like amount of dye, adsorbent quantity, pH, reaction time and temperature were varied to determine optimum conditions for the effective removal of safranin O dye. Freundlich, Langmuir and Temkin isotherms correlated with investigational results to study the decolourization mechanism. In addition, the kinetic studies were also performed [13].

RESULTS AND DISCUSSION

UV-Vis absorption studies: When an aqueous silver nitrate solution was added to *Pongamia pinnata* leaf extract, the colour changed from light brown to a more characteristic reddish brown, supporting the formation of AgNPs. The formation of AgNPs was confirmed by the colour shift caused by the surface plasmon resonance (SPR) phenomenon, which exhibited an absorbance peak at 426 nm which was absent in leaf extract (Fig. 1). Thus, *Pongamia pinnata extract* assists in the reduction of silver ions to the metallic form [12,14].

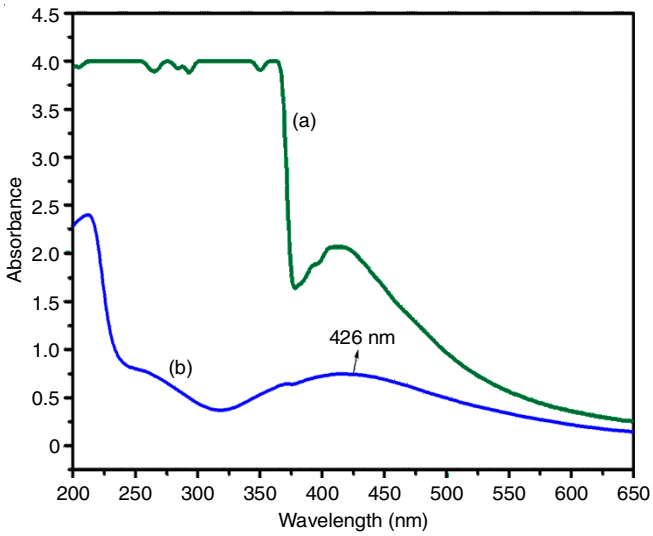

Fig. 1. UV-visible absorbance spectra of (a) *Pongamia pinnata* leaf extract and (b) AgNPs

FT-IR studies: A typical FTIR spectrum (Fig. 2) shows intense bands at 3491 and 3436 cm^{-1} are due to the O-H stretching vibrations. The peaks at 2084 cm^{-1} denotes the C-H stretching, while the peaks at 2924 and 2850 cm^{-1} attributes to the C-H asymmetrical and symmetrical stretching vibrations of CH_2 groups present in the sample. The peaks at 1642 and 1638 cm^{-1} resembled to the amide-I ascending from the C=O of proteins, while the peaks at 1387 and 1382 cm^{-1} can be attributed due to the C=O stretching vibrations of phenolic compounds. The weak bands at 1098 and 1114 cm^{-1} signifies the C-O stretching vibrations. At last, the peak at 776 cm^{-1} is due to CH_2 rocking. The suppression of bands in the aforementioned locations indicates that the Ag^+ ions have successfully dissociated into atoms, resulting in a stable sample [15,16].

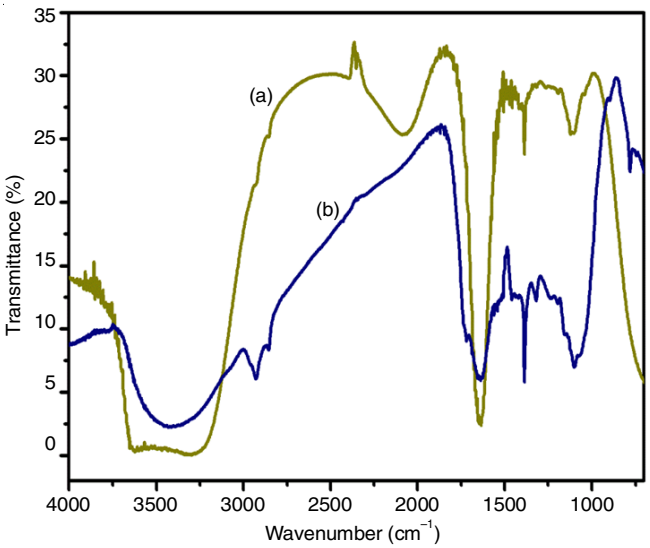

Fig. 2. FTIR spectra of (a) *Pongamia pinnata* leaf extract and (b) AgNPs

Structural studies: The XRD analysis was accomplished to regulate the crystallite size of the synthesized AgNPs. Fig. 3 corresponds to the XRD pattern of *Pongamia pinnata* leaf extract based AgNPs. Peaks at 2θ = 38.27º, 44.31º, 64.03º and 77.83º depicts the monoclinic phase of AgNPs with planes (111), (200), (220) and (311), respectively [17]. Absence of other peaks denotes that there is no impurity present in the sample. Broadening of peaks illustrates the reduction in crystallite size. Crystallite size was premeditated using Schererr's equation:

$$D = \frac{k\lambda}{\beta \cos\theta} \quad (1)$$

where, k represents shape factor and is about to be 0.89, θ is the diffraction angle, β denotes full width at half maximum and λ denotes wavelength of X-ray Cu*K*α radiation (0.154 nm); mean crystallite size was 24.84 nm.

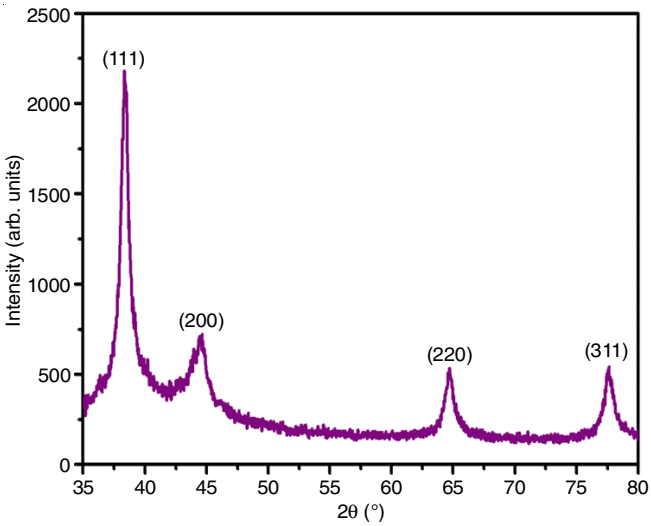

Fig. 3. XRD spectrum of green synthesized AgNPs

Dynamic light scattering (DLS) studies: The size of the nanoparticles is a crucial factor in the success of nanoparticle preparation. The diffusion limiting stoichiometry (DLS) method [18] uses the scattered light to assess the amount of diffusion. When sonicated in distilled water, the synthesized AgNPs made using environmentally friendly synthesis methods become widely dispersed throughout the liquid. Both the refractive index of 1.3328 (at 25 ºC) and the distribution viscosity of 0.896 (cP) are consistent with the analysis scenario. Size of synthesized AgNPs in the colloidal dispersion was found to be 75.8 nm (Fig. 4).

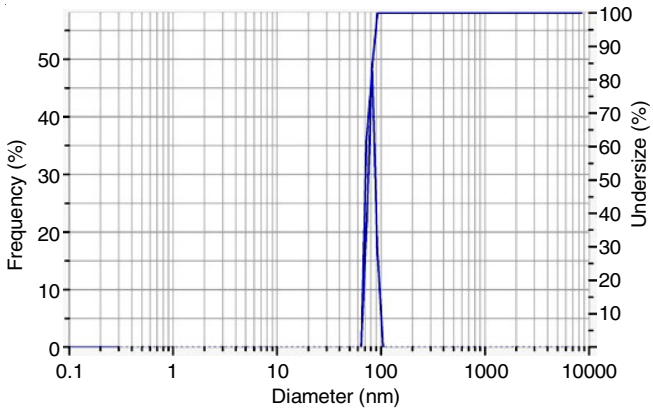

Fig. 4. DLS plot for green synthesized AgNPs

SEM studies: From the SEM images, the superficial shape (Fig. 5) were established as spherical in nature and size as 60-160 nm. Also the particles were slightly agglomerated. This could be due to the presence of the biomolecules present in the extract [19].

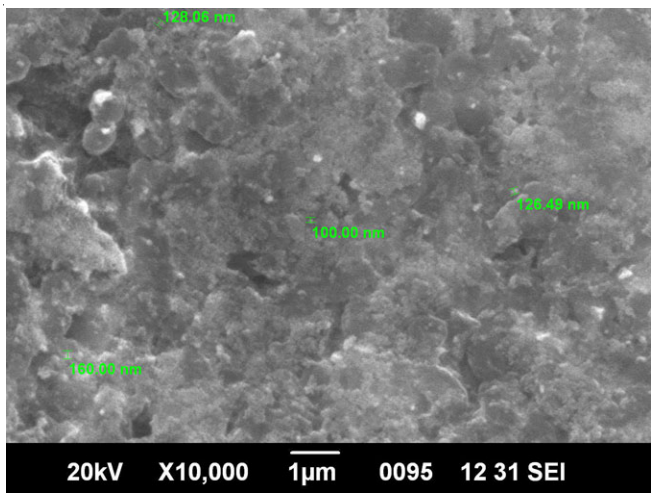

Fig. 5. SEM image of green synthesized AgNPs

TEM and SAED studies: From the TEM images (Fig. 6a), it was found that the synthesized AgNPs possess distorted spherical morphology with smooth surface. The particle size dispersal and average size distribution was calculated from Gaussian fitting of size distribution histogram (Fig. 6b). Particle distribution and size was around 10 to 100 nm whereas the ordinary particle size is 45.8 nm. Fig. 6c depicts the clear lattice fringes obtained from HRTEM analysis with springe arrangement of 0.24 nm, which represents to silver (111) [20]. The crystalline behaviour of the green synthesized AgNPs was

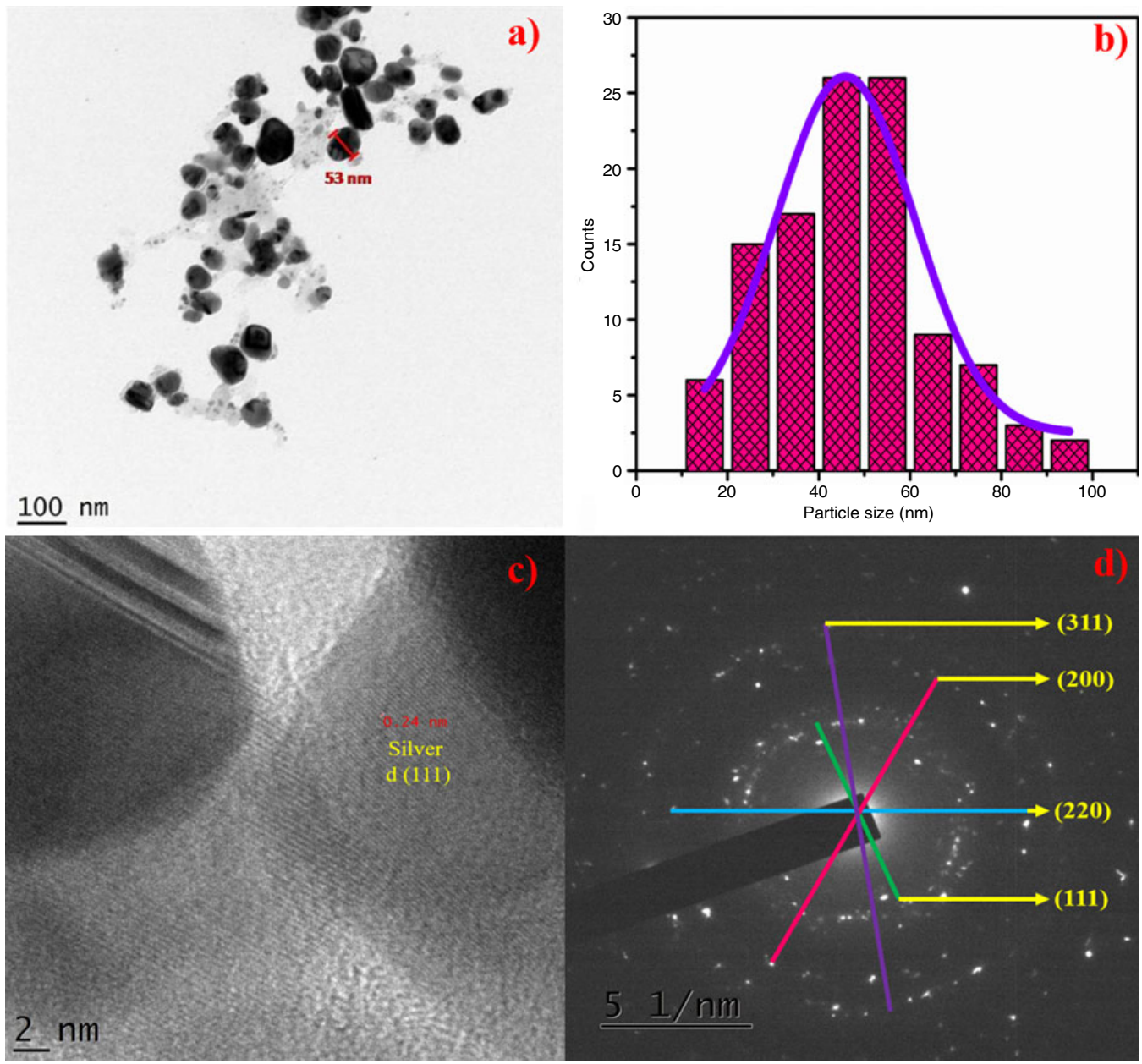

Fig. 6. (a) TEM image, (b) particle size histogram, (c) HRTEM image and (d) SAED pattern of green synthesized AgNPs

recognized by the presence of bright spots (Fig. 6d). The d-spacing obtained from SAED pattern is matched well with the d-spacing obtained from the XRD data.

Degradation of safranin O dye: The characteristic peak of safranin O dye got diminished upon treatment with the green synthesized AgNPs with constant stirring in mechanical shaker (Fig. 7). The percentage of dye removal was estimated using eqn. 2 [18]:

$$\text{Dye removal (\%)} = \frac{\text{Initial conc.} - \text{Final conc.}}{\text{Initial conc.}} \times 100 \quad (2)$$

Influence of amount of dye: Optimum concentration of dye is more important for effective dye removal. To estimate the optimum dye concentration we performed dye removal studies at five different dye concentrations of safranin O (10, 20, 30, 40 and 50 mg). It was found that the maximum dye degradation was achieved with the usage of 10 mg dye with 98.9% degradation efficiency (Fig. 8). When the dye concentration is increased, additional dye molecules gets accessible for triggering and more energy transmission is required. So, there is decrease in the infiltration of light to catalyst surface. Also, the generation of OH radicals is concentrated as the active spots are preoccupied by molecules of dye. In addition, when amount of dye upsurges, the necessity for catalyst also increases, which results in the increase of irradiation time. The relative amount of allowed radicals confronting dye reduces with enhanced dye concentration [21].

Influence of adsorbent loading: To estimate optimum loading of adsorbent, five different concentration of synthesized AgNPs (0.2, 0.4, 0.6, 0.8 and 1 g) were utilized for the

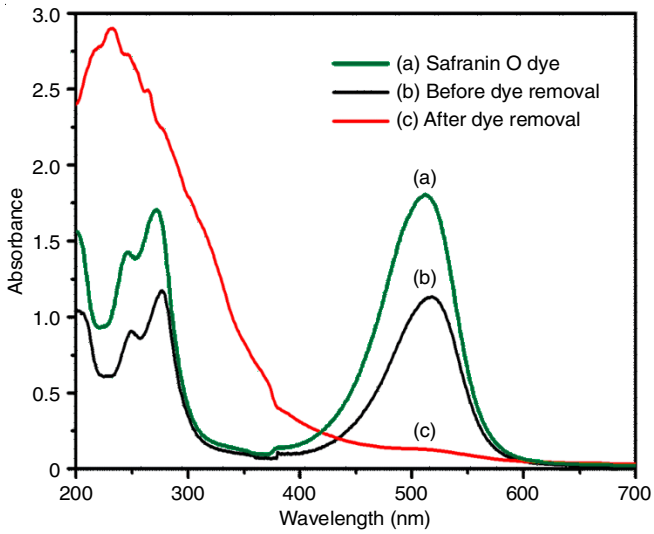

Fig. 7. Absorbance spectra of safranin O dye-before and after dye removal

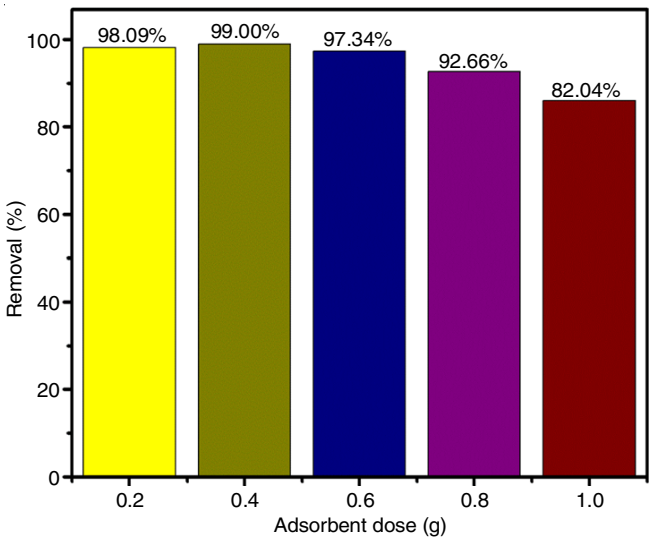

Fig. 9. Degradation plot of safranin O dye with varied adsorbent dosage

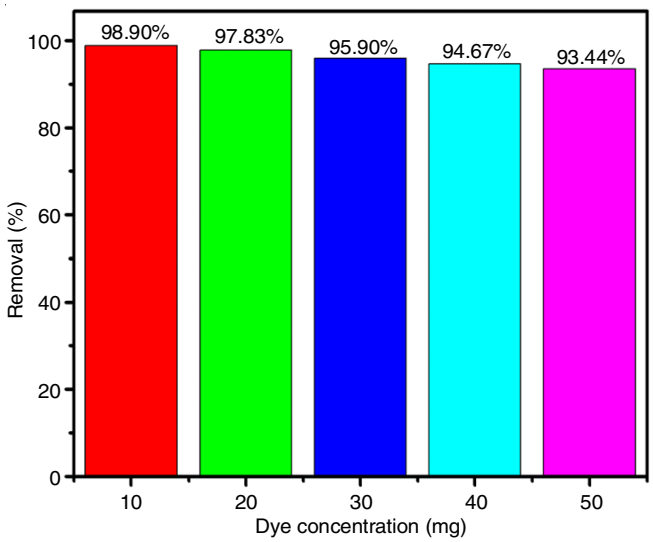

Fig. 8. Degradation plot of safranin O dye with varied dye concentration

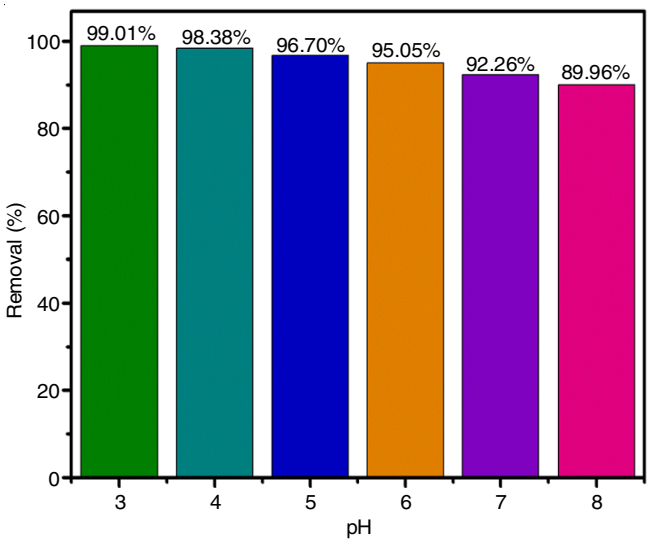

Fig. 10. Degradation plot of safranin O dye at different pH

degradation of safranin O dye. It was evaluated that maximum dye degradation (99%) was observed for 0.4 g of catalyst (Fig. 9). An increased in the catalyst concentration enhances the amount of photons adsorbed and subsequently the dye degradation rate is increased. Also, increase in catalyst amount enhances the solution opaqueness and it trails to a reduction in diffusion of light flux in reaction and hence reduces the degradation result. Moreover, the aggregated particles have improved particle-particle interactions since their surface area has been reduced [21].

Influence of pH: Dye degradation is generally attributed to $OH^{\bullet}$ attack, positive hole oxidizes straight, succeeded by decrease by e^{-} present at conduction band. All these aspects drastically relies on the substrate and pH. As a result, the effectiveness of six different pHs (pH = 3, 4, 5, 6, 7 and 8) in eliminating colour was examined. It was observed that safranin O degradation was maximum at pH = 3 with 99.01% degradation efficiency (Fig. 10). Hence, the optimum pH for safranin O degradation using green synthesized AgNPs was pH = 3. In alkaline conditions, the rate of disintegration slowed down marginally [21,22].

Influence of time: Optimum reaction time was studied by varying the contact time (30, 60, 90, 120 and 150 min). Better dye removal was observed at 30 min reaction time with 99% (Fig. 11). When reaction time was augmented, the efficiency of dye removal also decreased, which is due to the attachment of more organic materials on the apparent green synthesized AgNPs, while less amount of photons offered to grasp the exterior of the adsorbent, hence formation of $OH^{\bullet}$ radical is less resulting in the reduction in degradation efficiency [21].

Influence of temperature: To know optimum temperature for safranin O dye degradation we carried out at four different temperatures (298, 308, 318 and 328 K). We observed that safranin O dye degradation was maximum at 298 K with 98.62% degradation efficacy (Fig. 12). The reason is attributed at low temperature, desorption limits the reaction due to slow degradation on the surface and adsorption of the reactants. Whereas, at higher temperature, dissolved oxygen decreases the rate constant [21].

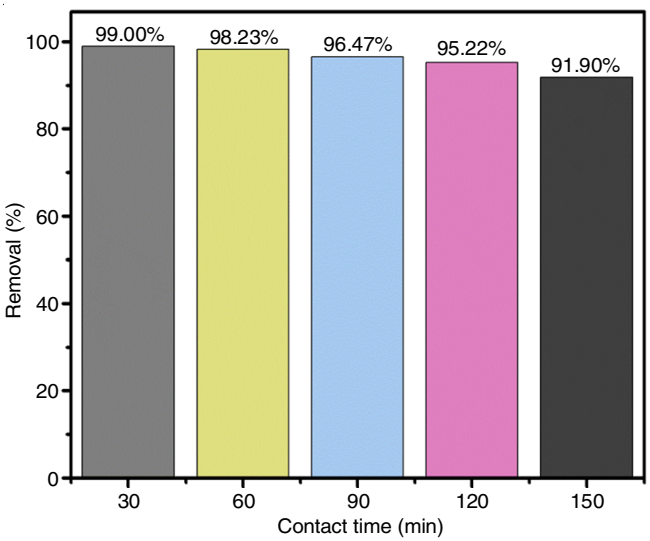

Fig. 11. Degradation plot of safranin O dye with varied contact time

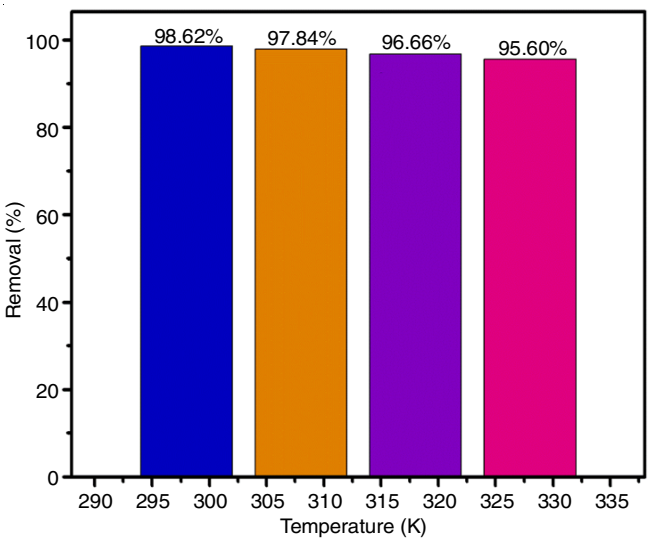

Fig. 12. Degradation plot of safranin O dye with varied temperature

Isotherm studies: Heterogeneous systems are denoted by a emperical equation of the Freundlich isotherm and its linear nature is represented by eqn. 3:

$$\log q_e = \log K_F + \frac{1}{n}\log C_e \quad (3)$$

where K_F is a constant linking the sorption ability and 1/n is an empirical factor related to the sorption intensity, which varies with the materials. Herein, m = 1/n = 0.4441 and n is 2.2517. The value of 1/n in the range 0 to 1 denotes good sorption ability of the synthesized AgNPs.Thus, the result of 1/n in this study indicates that the sorption of safranin O dye at the AgNPs was favourable and also indicates that the AgNPs have improved surface heterogeneity. Typically, the Freundlich isotherm defines a large surface exposure, signifying a large number of layers of sorption on the adsorbent layer, however this model has not predicted the adsorbent being saturated by the dye molecule [14].

$$C = \log K_F = 0.1349$$

$$K_F = \text{antilog } (0.1349) = 1.3642$$

$$K_F = 1.3642$$

Another adsorption isotherm, *i.e.* Langmuir isotherm is represented by eqn. 4:

$$\frac{1}{q_e} = \frac{1}{q_m K_L C_e} + \frac{1}{q_m} \quad (4)$$

where q_m is the monolayer sorption capacity of the sorbent (mg/g), q_e is the equilibrium dye concentration on the sorbent (mg/g), C_e is the equilibrium concentration of dye in the solution (mg/L) and K_L is the Langmuir sorption constant (l/mg) related to the free energy of sorption.

Langmuir adsorption isotherm proposes a single layer coverage of the adsorbed molecules. The values of the constants q_m and b are given in Table-1. An high R^2 value (0.9744) is the distinctive feature of best sorbent. This behaviour suggests that both homogeneous and heterogeneous sites are involved in the latter stages of the sorption process. Thus, the Langmuir isotherm suggests that the dynamic sites may be distributed in the same unilayer, suggesting the possibility of chemisorption over ion-exchange as the adsorption mechanism [14].

TABLE-1
ADSORPTION ISOTHERM PARAMETERS
FOR SAFRANIN O DYE

Adsorption isotherm	Parameters	Obtained values
Freundlich isotherm	K_F (mg/g)	1.3642
	1/n	0.4441
	n	2.2517
	R^2	0.9982
Langmuir isotherm	K_L (mg^{-1})	3.0571
	q_m (mg/g)	2.0012
	R_L	0.0316
	R^2	0.9744
Temkin isotherm	K_T (mol/g)	19.4249
	B_T (mol/kJ)	0.5143
	R^2	0.9513

Temkin adsorption isotherm model is applicable for the interactions between the adsorbent and the adsorbate and is represented by eqn. 5. This adsorption isotherm is based on the hypothesis that the adsorption of adsorbate is uniformly spread and the heat of adsorption decreases linearly with the exposure of molecules in layer due to the adsorbate-adsorbate interaction.

$$Q_e = \frac{RT}{b_T}\ln K_T + \left(\frac{RT}{b_T}\right)\ln C_e \quad (5)$$

where constant B = RT/b, which is correlated to the heat of sorption, R is the universal gas constant (kJ/mol K), T is the temperature (K), b is the variation of sorption energy (J/mol) and K_T is the equilibrium binding constant (L/mg) agreeing to greater binding energy. The values of constants B and K_T are given in Table-1.

Degradation kinetic studies: Safranin O dye degradation followed first order and second order kinetics. The first and second order reaction kinetic plots are depicted in Fig. 13. The first and second order kinetics exhibited R^2 values of 0.7568

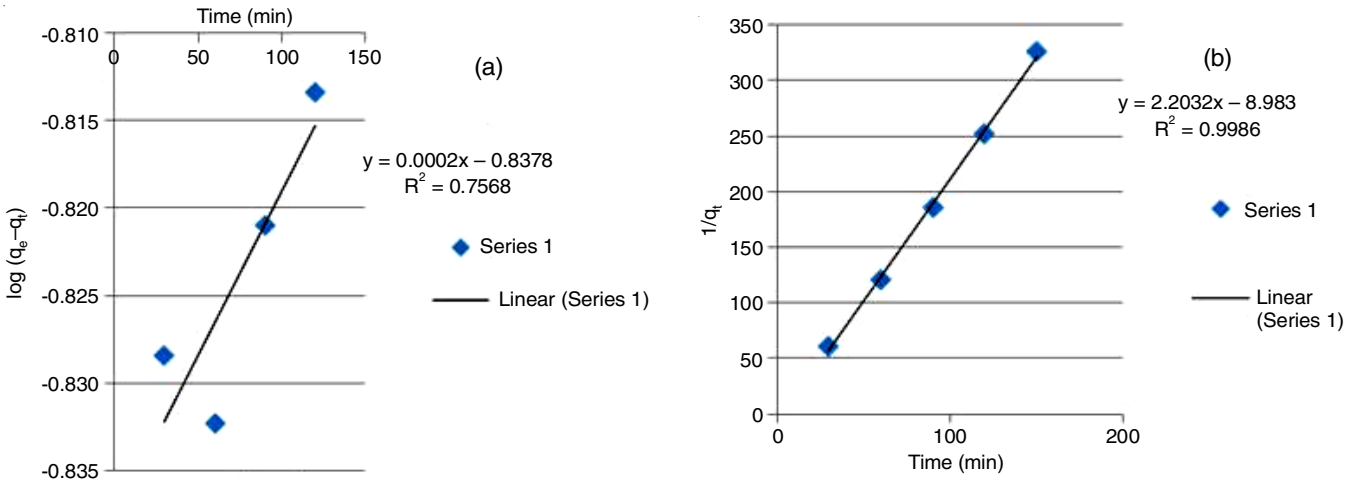

Fig. 13. Plots of (a) pseudo-first order kinetics and (b) pseudo-second order kinetics

and 0.9986, respectively. While comparing the adsorption nature of safranin O dye at the green synthesised AgNPs, the R^2 value for the pseudo-first order model (0.7568) is lower to the pseudo-second order (0.9986), but closer to the value of 1, therefore the pseudo-second order model is more appropriate.

Comparison studies: Table-2 depicts the comparative results of safranin O dye removal using other reported nanomaterial as adsorbents. As observed, green synthesized AgNPs exhibited the better safranin O dye removal efficiency within 30 min. Thus, the synthetic green route adopted for the AgNPs under the optimized conditions in the present work makes it as a potential candidate for safranin O dye removal with enhanced efficiency.

Conclusion

Herein, the silver nanoparticles was synthesized through green route using *Pongamia pinnata* leaf extract, where theleaf extract served as a stabilising and reducing agent. The synthesized nanoparticles was characterized through UV-Vis, FTIR, XRD, DLS, SEM, TEM and SAED techniques. From UV-Vis spectrum, the surface plasmon resonance phenomenon was observed with an absorbance peak at 426 nm. By means of Scherrer's equation, the average crystallite size was estimated to be 24.84 nm. Appearance of single peak in DLS plot confirms the high purity of the green synthesized AgNPs. The microscopic techniques proved the spherical shape of AgNPs, whereas the bright spots in the SAED pattern confirmed the high crystallinity of the synthesized silver nanoparticles. The degradation efficiency of the synthesized AgNPs towards Safranin O dye was achieved upto 99.01% under the optimized conditions at 298 K. The batch experimental results well fitted to linear isotherms.

ACKNOWLEDGEMENTS

The authors thank STIC, CUSAT, Cochin, India for conducting the electron microscopic studies. Thanks are also due to Department of Chemistry, IIT Madras, Chennai and Analytical Chemistry Department, Madras University, Chennai, India for rendering XRD and DLS analysis, respectively.

CONFLICT OF INTEREST

The authors declare that there is no conflict of interests regarding the publication of this article.

REFERENCES

1. I. Kovács, G. Veréb, S. Kertész, C. Hodúr and Z. László, *Environ. Sci. Pollut. Res. Int.*, **25**, 34912 (2018); https://doi.org/10.1007/s11356-017-0998-7
2. R. Razavi, M. Amiri, H.A. Alshamsi, T. Eslaminejad and M. Salavati-Niasari, *Arab. J. Chem.*, **14**, 103323 (2021); https://doi.org/10.1016/j.arabjc.2021.103323
3. W. Cheng, S.G. Wang, L. Lu, W.X. Gong, X.W. Liu, B.Y. Gao and H.Y. Zhang, *Biochem. Eng. J.*, **39**, 538 (2008); https://doi.org/10.1016/j.bej.2007.10.016

TABLE-2
COMPARATIVE RESULTS OF SAFRANIN O DYE REMOVAL USING VARIOUS NANOPARTICLES

Type of nanoparticles (NPs)	Method of synthesis	Adsorption capacities	Time (min)	Reference
Lignin NPs	Copolymerization reaction	99 mg/g	100	[23]
SiO_2 and TiO_2 capped Ag_2S nanocomposite	Hydrothermal method	91.38%	–	[24]
CuS NO	Solid state reaction	22.00%	180	[25]
CuO NPs	Green synthesis	189.54 mg/g	480	[26]
Fe_3O_4 NPs	Chemical precipitation	769.23 mg/g	–	[27]
TiO_2 nanopowder	Commercial	88.176%	100	[28]
Fe_3O_4/Ag nanocomposite	Co-Precipitation	46.3 mg/g	–	[29]
Agar-graphene oxide hydrogel	Jellification process	100 mg/g	–	[30]
ZnO nanorods-loaded activated carbon	Ultrasonic method	32.06 mg/g	–	[31]
AgNPs	Green synthesis	99.01%	30	This work

4. J. Singh and A.S. Dhaliwal, *Environ. Technol.*, **41**, 1520 (2020); https://doi.org/10.1080/09593330.2018.1540663
5. G. Ganapathy Selvam and K. Sivakumar, *Appl. Nanosci.*, **5**, 617 (2015); https://doi.org/10.1007/s13204-014-0356-8
6. A. Fiorati, A. Bellingeri, C. Punta, I. Corsi and I. Venditti, *Polymers*, **12**, 1635 (2020); https://doi.org/10.3390/polym12081635
7. D. Garibo, H.A. Borbón-Nuñez, J.N.D. de León, E. García Mendoza, I. Estrada, Y. Toledano-Magaña, H. Tiznado, M. Ovalle-Marroquin, A.G. Soto-Ramos, A. Blanco, J.A. Rodríguez, O.A. Romo, L.A. Chávez-Almazán and A. Susarrey-Arce, *Sci. Rep.*, **10**, 12805 (2020); https://doi.org/10.1038/s41598-020-69606-7
8. A. Rautela, J. Rani and M. Debnath (Das), *J. Anal. Sci. Technol.*, **10**, 5 (2019); https://doi.org/10.1186/s40543-018-0163-z
9. K.V. Usharani, D. Naik and R.L. Manjunatha, *J. Pharmacogn. Phytochem.*, **8**, 2181 (2019).
10. A.G. Fugare, R.V. Shete, V.S. Adak and G. Krishna Murthy, *J. Drug Deliv. Ther.*, **11(1-s)**, 207 (2021); https://doi.org/10.22270/jddt.v11i1-s.4522
11. S.P.S. Sri and M. George, *J. Mater. NanoSci.*, **8**, 1 (2021).
12. A. Roy, O. Bulut, S. Some, A.K. Mandal and M.D. Yilmaz, *RSC Adv.*, **9**, 2673 (2019); https://doi.org/10.1039/C8RA08982E
13. B. Ekka, M.K. Sahu, R.K. Patel and P. Dash, *Water Resour. Ind.*, **22**, 100071 (2019); https://doi.org/10.1016/j.wri.2016.08.001
14. A.M.K. Pandian, C. Karthikeyan and M. Rajasimman, *Nanotechnol. Environ. Eng.*, **2**, 2 (2017); https://doi.org/10.1007/s41204-016-0013-4
15. Naik, G.S. Gowreeswari, Y. Singh, R. Satyavathi, S.S. Daravath and P.R. Reddy, *Adv. Entomol.*, **2**, 93 (2014); https://doi.org/10.4236/ae.2014.22016
16. C. Karthik, S. Suresh, G. Sneha Mirulalini and S. Kavitha, *Inorg. Nano-Metal Chem.*, **50**, 606 (2020); https://doi.org/10.1080/24701556.2020.1723025
17. M. Shu, F. He, Z. Li, X. Zhu, Y. Ma, Z. Zhou, Z. Yang, F. Gao and M. Zeng, *Nanoscale Res. Lett.*, **15**, 14 (2020); https://doi.org/10.1186/s11671-019-3244-z
18. V.S.P.S. Sri, A. Manikandan, M. Mathankumar, R. Tamizhselvi, M. George, K. Murugaiah, H.A. Kashmery, S.A. Al-Zahrani, M. Puttegowda, A. Khan and A.M. Asiri, *J. Mater. Res. Technol.*, **15**, 99 (2021); https://doi.org/10.1016/j.jmrt.2021.07.145
19. S.P. Sakthi Sri, J. Taj and M. George, *J. Surfin.*, **20**, 100609 (2020); https://doi.org/10.1016/j.surfin.2020.100609
20. G. Shruthi, K.S. Prasad, T.P. Vinod, V. Balamurugan and C. Shivamallu, *ChemistrySelect*, **2**, 10354 (2017); https://doi.org/10.1002/slct.201702257
21. K.M. Reza, A. Kurny and F. Gulshan, *Appl. Water Sci.*, **7**, 1569 (2017); https://doi.org/10.1007/s13201-015-0367-y
22. C.V. Rao, A.S. Giri, V.V. Goud and A.K. Golder, *Int. J. Ind. Chem.*, **7**, 71 (2016); https://doi.org/10.1007/s40090-015-0060-x
23. J. Azimvand, Kh. Didehban and S.A. Mirshokraie, *Adsorption Sci. Technol.*, **36**, 1422 (2018); https://doi.org/10.1177/0263617418777836
24. D. Ayodhya and G. Veerabhadram, *J. Environ. Chem. Eng.*, **6**, 311 (2018); https://doi.org/10.1016/j.jece.2017.11.071
25. F. Siddique, M.A. Rafiq, M.F. Afsar, M.M. Hasan and M.M. Chaudhry, *J. Mater. Sci.: Mater. Electron.*, **29**, 19180 (2018); https://doi.org/10.1007/s10854-018-0044-7
26. T.B. Vidovix, H.B. Quesada, R. Bergamasco, M.F. Vieira and A.M.S. Vieira, *Environ. Technol.*, **43**, 3047 (2022); https://doi.org/10.1080/09593330.2021.1914180
27. S. Shariati, M. Faraji, Y. Yamini and A.A. Rajabi, *Desalination*, **270**, 160 (2011); https://doi.org/10.1016/j.desal.2010.11.040
28. K.M. Jasim and L.M. Ahmed, *Mater. Sci. Eng.*, **571**, 1 (2019); https://doi.org/10.1088/1757-899X/571/1/012064
29. M.A. Salem, I.A. Salem, H.M. Zaki and A.M. El-Sawy, *Egypt. J. Petrol.*, **31**, 39 (2022); https://doi.org/10.1016/j.ejpe.2022.05.002
30. C.M.B. de Araujo, G. Wernke, M.G. Ghislandi, A. Diório, M.F. Vieira, R. Bergamasco, M.A. da Motta-Sobrinho and A.E. Rodrigues, *Environ. Res.*, **216**, 114425 (2023); https://doi.org/10.1016/j.envres.2022.114425
31. E. Sharifpour, M. Ghaedi, F.N. Azad, K. Dashtian, H. Hadadi and M.K. Purkait, *Appl. Organometal. Chem.*, **32**, e4099 (2017); https://doi.org/10.1002/aoc.4099